optical clock signal now showed evidence of ~40 ps of jitter and the tolerance to SP-LD bias was more critical. In the RF spectrum the modulation components either side of the clock frequency were now only suppressed by ~20 dB and we believe this poor suppression is due to the format of the input signal to the SP-LD. In RZ data and optical-time-division-multiplexed data the optical '1's are of similar time duration to the pulses naturally emitted from the SP-LD. In NRZ format this is not the case and so a long series of '1's in the input signal can alter the pulsation frequency due to the change in the carrier lifetimes associated with the high stimulated emission rate. This effect is clearly seen in Fig. 3 which shows the increase in selfpulsation frequency of the SP-LD when a CW −12·2 dBm signal was injected into the device at two different wavelengths. The increase in frequency only occurs when the input wavelength overlaps the FP mode spectrum of the SP-LD, i.e. at different bias currents. This sweeping of the natural SP-LD pulsation frequency due to the input signal power allows other modulation components in the data spectrum to resonate with the SP-LD which results in the poor supression which in turn produces the observed jitter in the output clock pulses. This hypothesis is partly validated by the observation that a larger relaxation transient to the NLOA output pulses (Fig. 2*b*) resulted in a better synchronisation of the SP-LD output. An equal amount of jitter was observed for a 2^{23}-1 pattern.

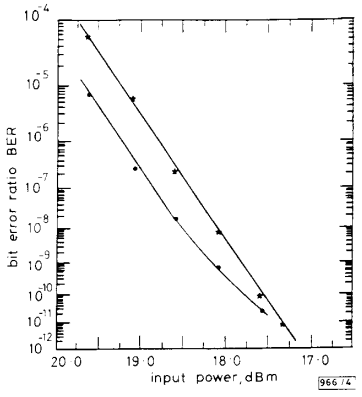

Fig. 4 *Variation of bit-error-ratio optical receiver input power using the transmitter clock and extracted optical clock, 3·2 Gbit/s NRZ (1010)*

* with transmitter clock
• with optical clock

Discussion: Although the NLOA generates the clock component to the modulation spectrum the optical power dependence of the SP-LD pulsation frequency prevents satisfactory operation with NRZ pseudorandom data. The suppression ratio between the clock component and the other modulation components needs to be increased. Satisfactory operation could be obtained if the SP-LD output were further filtered to ensure that the clock component dominates. One way of achieving this would be to use electrical techniques, such as a phase-locked-loop, but this would significantly reduce the bit-rate insensitivity of the clock extraction circuit. An alternative way may be to cascade two SP-LD devices whose natural pulsation frequencies were locked together. The first SP-LD coarsely filters the clock component from the NLOA output modulation spectrum and provides a pulse format for the second SP-LD which can then discriminate the clock frequency from the adjacent modulation components. For this configuration to work, the jitter transfer and tolerance of the SP-LD will have to be very good and further work is required to determine if this approach can be implemented. The complications of such a clock extraction configuration could be eased by integration of the two-contact devices with passive waveguide technology.

Conclusions: We have demonstrated all-optical clock recovery from a 3·2 Gbit/s NRZ 1010.. data sequence using a nonlinear optical amplifier to generate the missing clock component which then locked the output of a selfpulsating laser. BER measurements showed that the resulting clock signal was extremely pure and stable. Experimentation with NRZ pseudorandom data showed the presence of jitter induced by the power dependence of the SP-LD pulsation frequency. Further work will determine whether a full NRZ system configuration can be implemented.

Acknowledgments: The author wishes to thank his colleagues in both the Devices Research and Main Networks Divisions for valuable discussions and continued support.

11th May 1992

P. E. Barnsley (*BT Laboratories, Martlesham Heath, Ipswich, IP5 7RE, United Kingdom*)

References

1 JINNO, M., MATSUMOTO, T.: 'Optical retiming regenerator using 1·5 μm wavelength multielectrode DFB LD's', *Electron. Lett.* 1989, **25**, (20), pp. 1332–1333
2 JINNO, M., MATSUMOTO, T., and KOGA, M.: 'All-optical timing extraction using an optical tank circuit', *Photonics Technol. Lett.* 1990, **2**, (3), pp. 203–204
3 BARNSLEY, P. E., WICKENS, G. E., WICKES, H. J., and SPIRIT, D. M.: 'A 4 × 5 Gb/s transmission system with all-optical clock recovery', *Photonics Technol. Lett.*, 1992, **4**, (1), pp. 83–86
4 BARNSLEY, P. E., MARSHALL, I. W., FIDDYMENT, P. J., and ROBERTSON, M. J.: 'Absorptive nonlinear semiconductor devices for fast optical switching'. SPIE Vol 1378 Optically activated switching, 1990, pp. 116–126
5 BARNSLEY, P. E., and FIDDYMENT, P. J.: 'Clock extraction using saturable absorption in a semiconductor nonlinear optical amplifier', *Photonics Technol. Lett.*, 1991, **3**, (9) pp. 832–834

COLLINEAR BEAM ACOUSTO-OPTIC TUNABLE FILTERS

I. C. Chang

Indexing terms: Optical filters, Acousto-optical devices

A new type of noncollinear acousto-optic tunable filter (AOTF) suitable for fibre optic communication is described. The AOTF interaction geometry offers the advantages of narrow bandwidth and low drive power. Theoretical analysis of the TeO_2 filter shows that optical passband of 1 nm and drive power of 12 mW are obtainable.

The acousto-optic tunable filter (AOTF) is an electronically tunable optical filter that operates on the principle of acousto-optic diffraction in a birefringent crystal. Depending on the directions of the optical and acoustic wave vectors, there are the collinear [1], and noncollinear [2] types of AOTF. A significant feature of both types of AOTF is their large angular aperture while maintaining narrow spectral bandpass. This feature is the result of the design criterion that the tangents to the incident and diffracted wave vector surfaces be parallel [2]. The large angular aperture characteristic is particularly important in optical imaging sensor applications [3].

Recently there has been renewed interest in the development of collinear AOTFs. In a series of papers, Cheung *et al.* [4–6] have reported progress of integrated optic type AOTFs and their applications to dense wavelength division multiplexing (WDM) networks. For this type of application the optical beams are collimated, thus the parallel tangents condition can be relaxed.

This Letter describes a new type of noncollinear AOTF where the acoustic beam (i.e. group velocity direction) is collinear with the incident optical beam [7]. Fig. 1 shows the schematic diagram of a collinear beam AOTF. To minimise wavelength dispersion, an ordinary polarisation is chosen for the incident optical beam. The acoustic wave launched from the transducer is reflected from the prism surface which is chosen so that the acoustic group velocity is collinear with the incident ordinary ray. When the momentum matching condition is satisfied, an extraordinarily polarised diffracted optical beam at the passband wavelength will be generated in the crystal. The diffracted narrowband optical beams coupled out of the prism surface may be selected using polarisers or spatial separations.

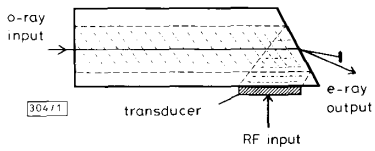

Fig. 1 *Schematic diagram of collinear beam AOTF*

A simple analysis of the collinear beam AOTF based on small fractional birefringence approximation is derived as follows. The directions of the optical and acoustic waves are related by the collinearity requriement, i.e.

$$\theta_g = \theta_0 \tag{1}$$

where θ_0 and θ_g are the polar angles of the optical ray and the acoustic group velocity, respectively. In a trigonal or tetragonal crystal the acoustic wave direction is given by

$$\tan \theta_a = (C_{14} - C_{44} \tan \theta_g)/(C_{14} \tan \theta_g - C_{66}) \tag{2}$$

From the diagram of optical and acoustic wave vectors, the momentum mismatch Δk can be obtained:

$$\Delta k/2\pi = (\Delta n/\lambda_0) \sin^2\theta_0 - (f_a/V) \cos(\theta_0 - \theta_a) \tag{3}$$

where Δn is the optical birefringence, λ_0 is the optical wavelength, and f_a and V are the frequency and velocity of the acoustic wave, respectively. At the centre wavelength the momentum-matching condition is satisfied, i.e. $\Delta k = 0$.

$$\lambda_0 = (V\ \Delta n \sin^2\theta_0)/(f_a \cos(\theta_0 - \theta_a)) \tag{4}$$

The diffracted light is spatially separated from the incident light. The angular separation is

$$\alpha = \Delta n \sin^2\theta_0 \tan(\theta_0 - \theta_a) \tag{5}$$

The spectral and angular bandwidths of the AOTF are determined from the phase mismatch $\Delta\phi = \Delta kL$, where L is the interaction length. From eqn. 3, the phase mismatch can be expressed as a function of wavelength and angular deviations

$$\Delta\phi = 2\pi L(\sin^2\theta_0/\lambda_0)[-(b\ \Delta\lambda/\lambda) + F\ \Delta n\ \Delta\theta] \tag{6}$$

where b is the dispersive constant [3] and $F = 2 \cot\theta_0 + \tan(\theta_0 - \theta_a)$. Letting $\Delta\phi = \pi$, the full widths at half maximum (FWHM) are

$$\Delta\lambda = \lambda_0^2/(bL \sin^2\theta_0) \tag{7}$$

$$\Delta\theta = (b\ \Delta\lambda)/(F\ \Delta n\lambda_0) \tag{8}$$

The angular aperture of the collinear beam AOTF is linearly proportional to the spectral bandwidth, and is therefore much smaller than that of the conventional AOTFs.

The drive power to achieve 100% diffraction efficiency is given by

$$P_a = (\lambda_0^2 A)/(2M_2 L^2) \tag{9}$$

where A is the acoustic beam size and M_2 is the acousto-optic figure of merit. Fig. 2 plots M_2 (relative to fused silica) of a collinear beam TeO_2 as a function of optical angle.

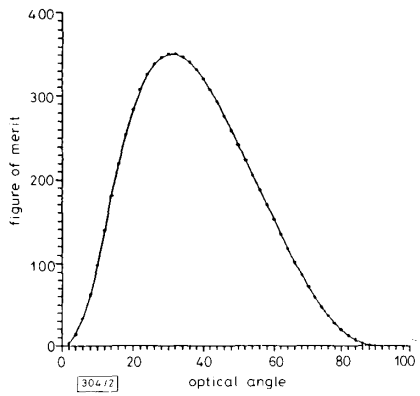

Fig. 2 *Figure of merit of TeO_2 collinear beam AOTF*

The most significant feature of the collinear beam AOTF is that it realises an extended interaction length and thus the advantages of narrow passband and low drive power. Consider the design of a collinear beam TeO_2 AOTF. Assume the following choice of parameter values: $\theta_0 = 55°$, $\theta_a = 86.6°$, $L = 2{\cdot}5$ cm, $A = 1$ mm^2. The calculated performance of the collinear AOTF is given in Table 1.

Table 1 CALCULATED PERFORMANCE OF COLLINEAR BEAM TeO_2 AOTF

Optical wavelength	1530 nm
Acoustic frequency	43 MHz
Deflection angle	3·2°
Passband FWHM	1 nm
Acoustic power	6 mw

Assume a 3 dB transducer insertion loss; the RF drive power is estimated to be 12 mW. This low drive power is comparable to that of an integrated AOTF using acoustic waveguides [8]. However, the bulk collinear beam AOTF has the advantage of lower optical insertion loss.

Acknowledgment: This work was sponsored by the Air Force Wright Laboratory.

6th March 1992

I. C. Chang (*Aurora Associates, Santa Clara, CA 95054, USA*)

References

1 HARRIS, S. E., and WALLACE, R. W.: 'Acousto-optic tunable filter', *J. Opt. Soc. Am.*, 1969, **59**, pp. 744–747
2 CHANG, I. C.: 'Noncollinear acousto-optic filter with large angular aperture', *Appl. Phys. Lett.*, 1974, **25**, pp. 370–372
3 CHANG, I. C.: 'Acousto-optic tunable filters', *Opt. Eng.*, 1981, **20**, pp. 824–829
4 HEFFNER, B. L. *et al.*: 'Integrated-optic acoustically-tunable infrared optic filter', *Electron. Lett.*, 1988, **24**, pp. 1562–1563
5 CHEUNG, K. W., *et al.*: 'Multiple channel operation of an integrated acousto-optic tunable filter', *Electron. Lett.*, 1989, **25**, pp. 375–376
6 CHEUNG, K. W.: 'Acousto-optic tunable filter in narrowband WDM networks: systems, issues, and network applications', *IEEE J. Sel. Areas Commun.*, 1990, **SAC-8**, pp. 1015–1025
7 CHANG, I. C.: 'Multiplexing for fiber-optic sensors'. Final Report for Contract No. F33615-91-C-1740, submitted to Wright Laboratory, WPAFB, December 1991
8 SMITH, D. A., and JOHNSON, J. J.: 'Low drive power integrated acousto optics filter on x-cut y propagating $LiNbO_3$', *IEEE Photonics Technol. Lett.* 1991, **3**, pp. 923–925